Supporting information

Dual Light Trapping and Water Repellent Effects of a Flexible Based Inverse Micro-Cone Array for Organic and Perovskite Solar Cells

Riski Titian Ginting,[a,b,†] Eun-Bi Jeon,[a,†] Jung-Mu Kim,[c] Won-Yong Jin,[a] and Jae-Wook Kang[*,a]

[a]Department of Flexible and Printable Electronics, Polymer Materials Fusion Research Center, Chonbuk National University, Jeonju 54896, Republic of Korea

[b]Department of Electrical Engineering, Universitas Prima Indonesia, Medan, North Sumatra, Indonesia

[c]Department of Electronic Engineering, Chonbuk National University, Jeonju 54896, Republic of Korea

[†]R.T. Ginting, and E.-B. Jeon made equal contribution to this paper.

*To whom correspondence should be addressed.

Prof. Jae-Wook Kang (E-mail: jwkang@jbnu.ac.kr)

The master templates were first ultrasonically cleaned with acetone and IPA, followed by a hydrophobically modified surface by OTS in a low-vacuum desiccator to replicate the templates. The surface morphology of the master template observed by AFM with an AR of 0.6 showed a micro-cone width and depth of 2.88 and 1.15 μm, respectively. Afterwards, a NOA 74 solution was dropped onto the template and a polyethylene (PET) film was attached onto the surface prior to UV curing for 15 min. Figure S1b depicts the large flexible TCEs without and without MCA. The photograph images clearly show the MCA-textured film, where rainbow-like colors appear on the MCA surfaces due to the strong light diffraction properties, as evidenced by light diffraction illuminated by green LED.
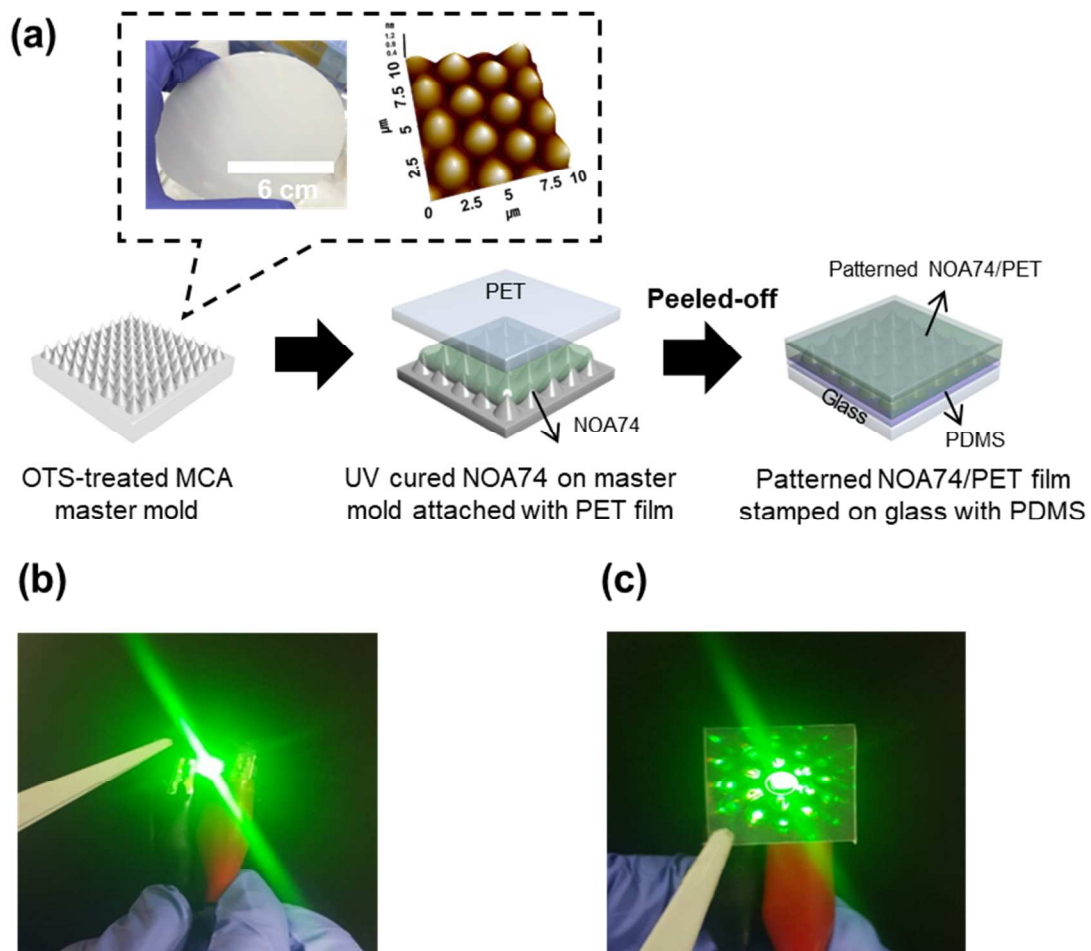
Figure S1. (a) Schematic illustration of the MCA replication process into PET from the master mold. The green light diffraction from the flexible TCEs film (b) without and (c) with MCA.
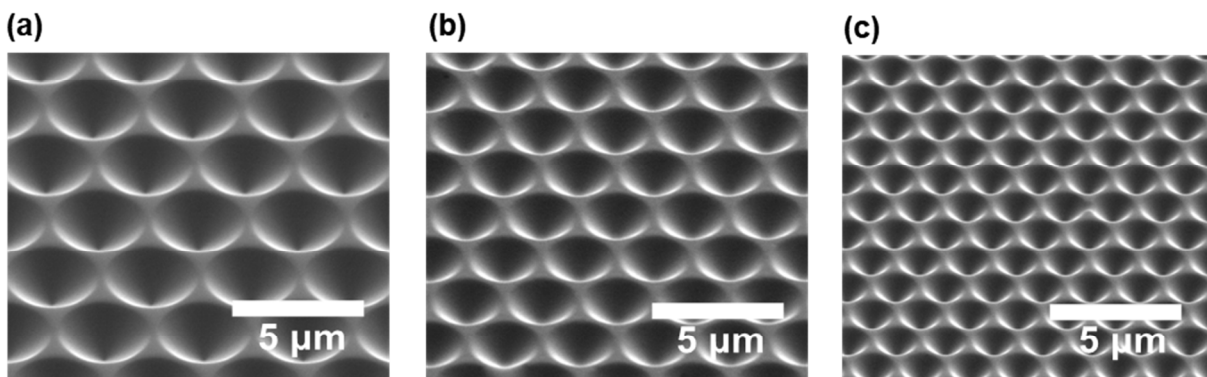
Figure S2. FESEM top images of patterned films after the imprinting process on NOA 74 with various ARs of (a) 0.5 (width 3.7 μm and depth 1.9 μm), (b) 0.6 (width 2.7 μm and depth 1.6 μm), and (c) 0.7 (width 1.8 μm and depth 1.3 μm).
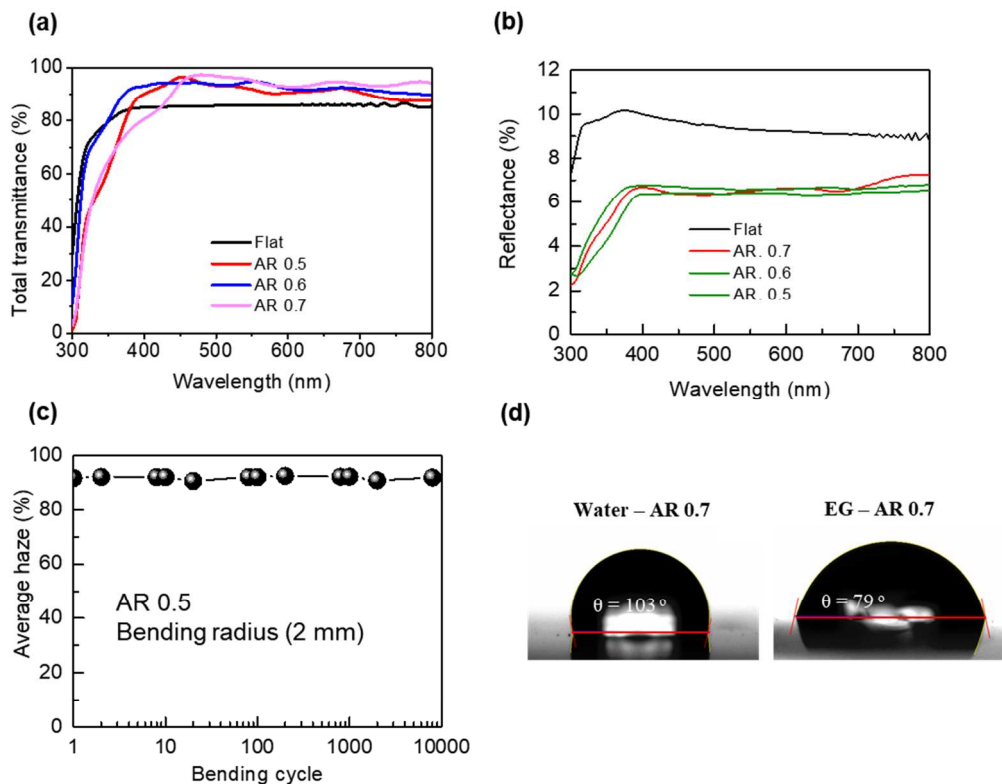
Figure S3. (a) Total transmittance of flat and flexible MCA substrates with various ARs, (b) reflectance spectra, (c) Average haze as a function of bending cycle up to 10,000 cycles at bending radius of 2 mm, and (d) photographs of the water and EG contact angles on the flexible MCA surface.
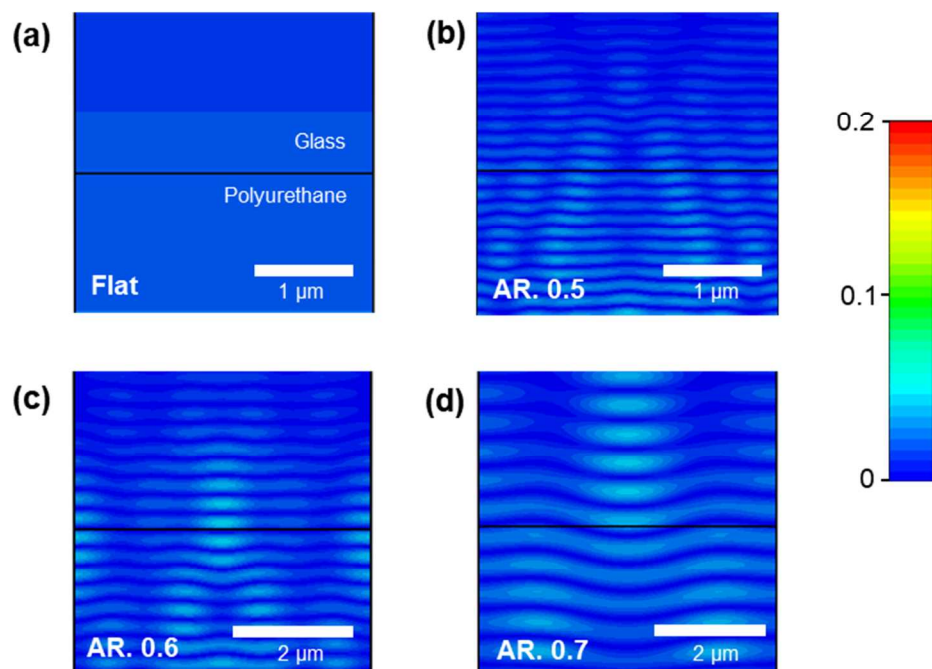
Figure S4. FIT simulation of the cross section of the NOA 74/glass interface for the (a) flat, (b) AR 0.5, (c) AR 0.6, and (d) AR 0.7 films at an incident wavelength of 530 nm.
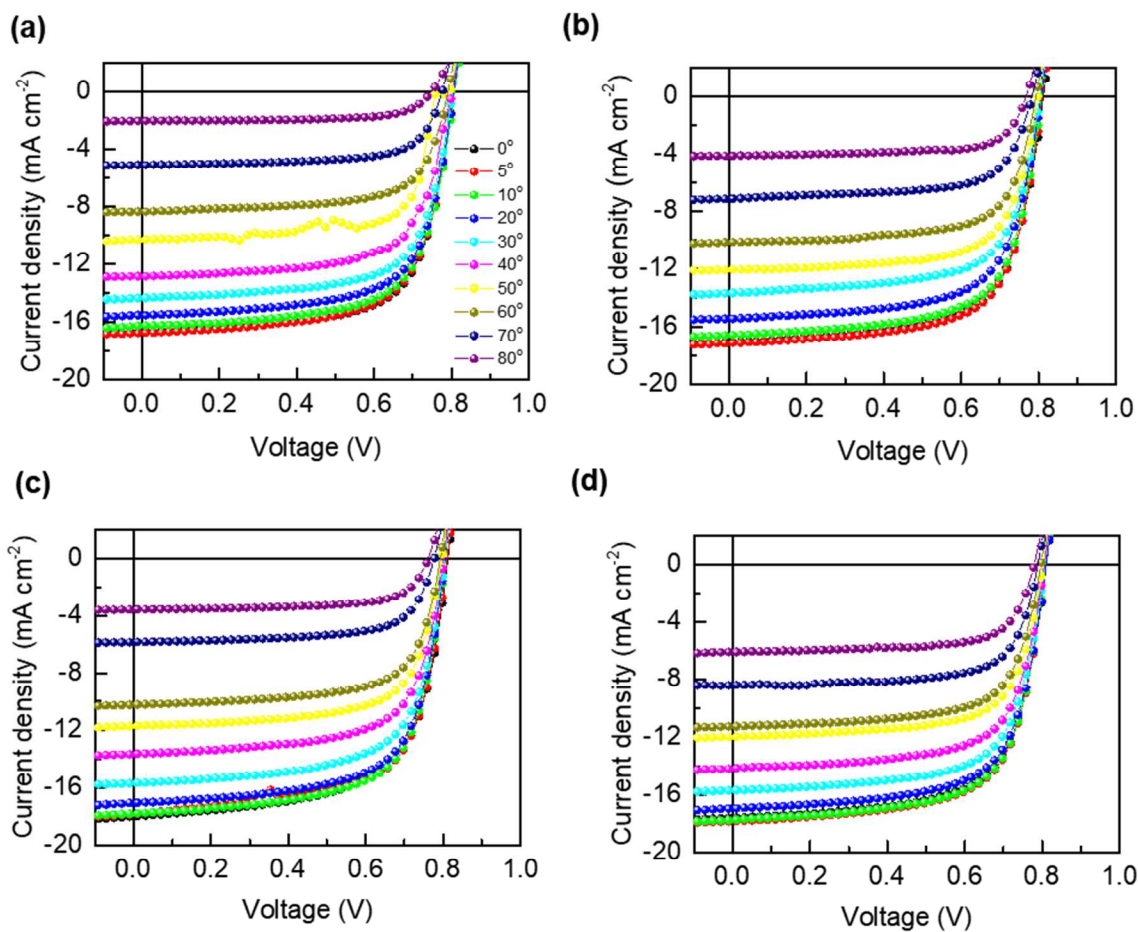
Figure S5. J-V characteristics at various incident angles for (a) flat, (b) AR 0.5, (c) AR 0.6, and (d) AR 0.7 MCA films attached on ITO/glass OSCs devices.
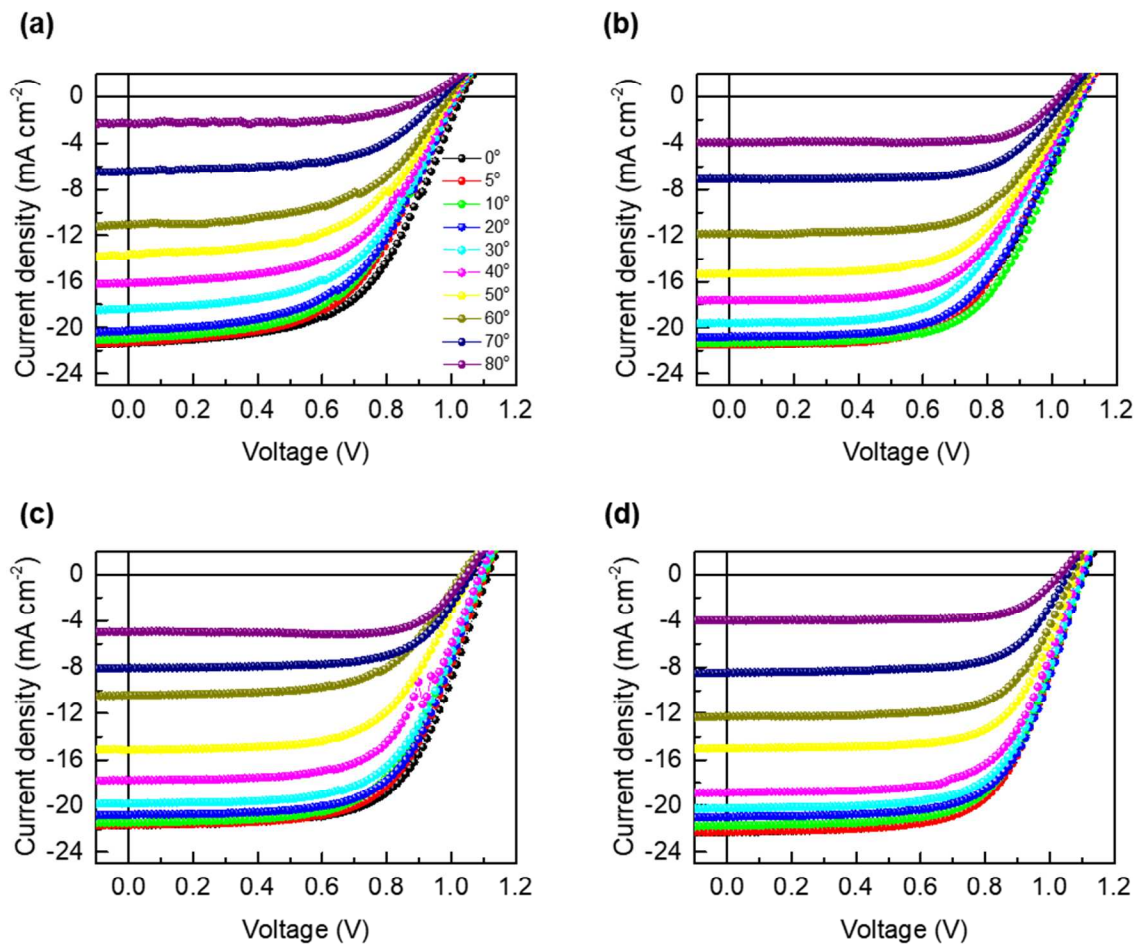
Figure S6. J-V characteristics at various incident angles for (a) flat, (b) AR 0.5, (c) AR 0.6, and (d) AR 0.7 MCA films attached on ITO/glass PSCs devices.

Using the results shown in Figures S5 and S6, the normalized photocurrent of OSCs and PSCs can be plotted as a function of the angular distribution to determine the energy density of the solar cells.
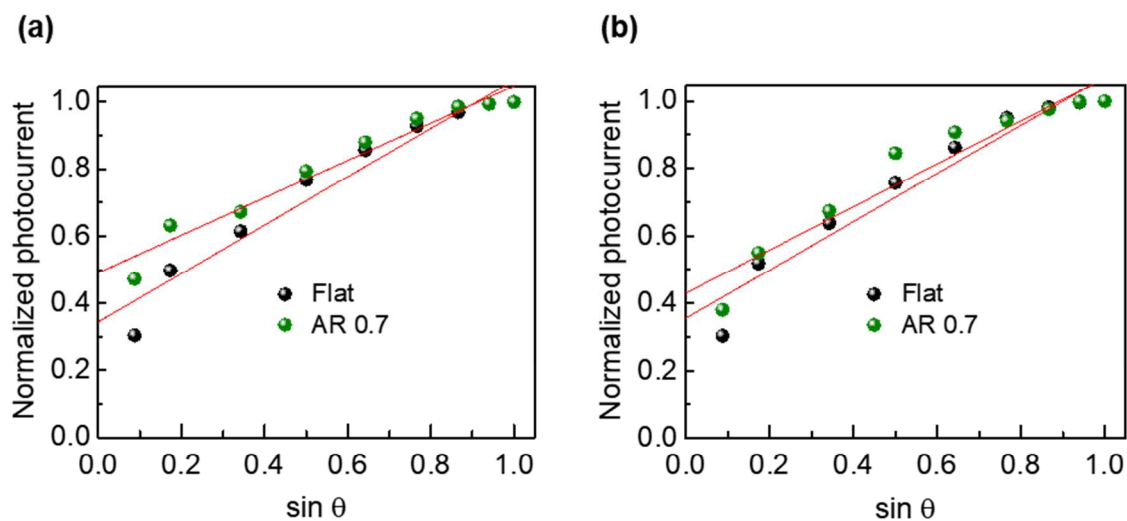

Figure S7. Normalized photocurrent as a function of the angular distributions of the (a) OSCs and (b) PSCs.
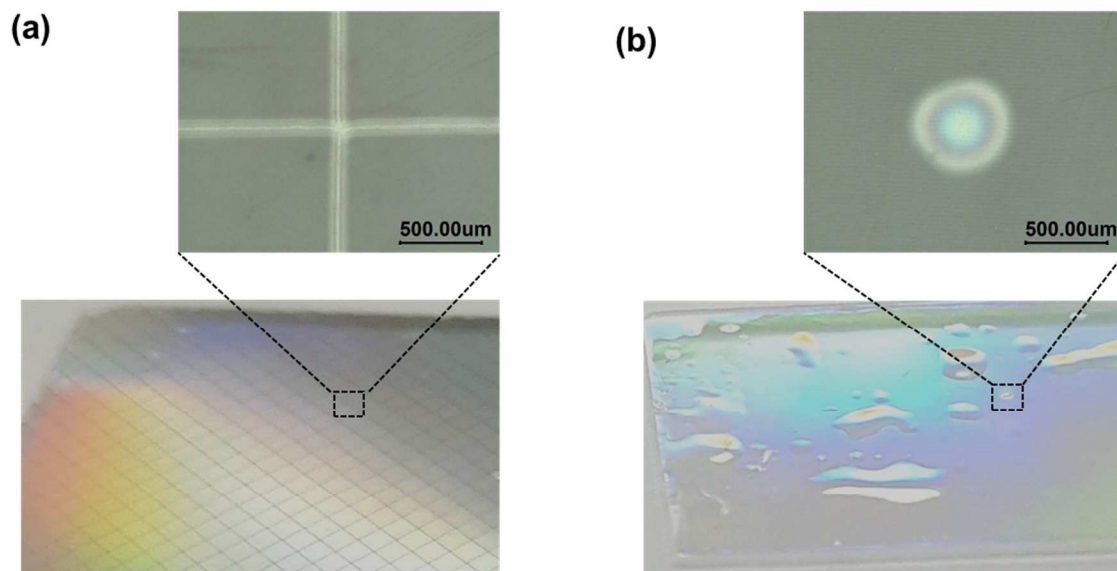
Figure S8. Microscopic images of (a) i-MCA-TCE film and (b) i-MCA film on the back of glass.

From Table 1, the average J_{sc} of respective flat and AR 0.7 film was determined at the normal incidence angle. In this calculation, we assumed that the power density of the sun is unchanged during daytime, where the OSCs and PSCs are placed parallel to the horizon line according to a previous publication.[1] We assume that during the autumnal or spring equinox, sunshine irradiates earth for 12 h (t). The total energy density generated by solar cells can be expressed as E= UIt =$U\int_0^{12} I(t) \cdot t\, dt$, where U is the voltage output (V_{oc}) and $I(t)$ is the photocurrent as a function of time. The normal incident of sunlight is 90° and $sin\theta = cos\left(\frac{t-12}{12}\pi\right)cos\varphi$, where θ is the incidence angle and φ is latitude. Another assumption is that the light intensity is constant for 12 h during daytime and therefore, the photocurrent densities (J_{sc}) of OSCs and PSCs for the flat and i-MCA-textured films can be expressed as $I = J_{sc}(m sin\theta+b)$, where m is the slope of linear fitting and b is the intercept of the normalized photocurrent.

OSCs:

$$I_{flat} = 16.3\left(0.34 + 0.72cos\left(\frac{t-12}{12}\pi\right)cos\varphi\right) \tag{S1}$$

$$I_{0.7} = 17.4\left(0.49 + 0.56cos\left(\frac{t-12}{12}\pi\right)cos\varphi\right) \tag{S2}$$

PSCs:

$$I_{flat} = 21.4\left(0.35 + 0.71cos\left(\frac{t-12}{12}\pi\right)cos\varphi\right) \tag{S3}$$

$$I_{0.7} = 22.9\left(0.43 + 0.63cos\left(\frac{t-12}{12}\pi\right)cos\varphi\right) \tag{S4}$$

The equations above were solved using integration by parts, where U is a constant with values of 0.78 V and 1.08 V with and without i-MCA for OSCs and PSCs, respectively. E (mWh cm^{-2}) can

be obtained by substituting Eqs. S1, S2, S3, and S4 into the integral mentioned above to obtain the following expressions.

OSCs:

$$E_{flat} = 312 + 267 \cos\varphi \tag{S5}$$

$$E_{0.7} = 613 + 284 \cos\varphi \tag{S6}$$

PSCs:

$$E_{flat} = 583 + 475 \cos\varphi \tag{S7}$$

$$E_{0.7} = 767 + 453 \cos\varphi \tag{S8}$$

Accordingly, the above expressions indicate that higher latitudes will increase the energy density of OSCs and PSCs. In the case of the high latitude of South Korea of 37°, the E values of the OSCs for flat and AR 0.7 films are 525 and 839 mWh cm^{-2}, while the values of the PSCs are 746 and 1,148 mWh cm^{-2}, respectively. Similarly, if the device was placed in Indonesia at a lower latitude of 6°, the E values of the OSCs for flat and AR 0.7 films are 576 and 894 mWh cm^{-2}, while the values of the PSCs are 837 and 1215 mWh cm^{-2}, respectively.

(a)

Ag
Al 4083
PTB7:PCBM
ZnO
PEDOT:PSS
Polyurethane (NOA 63)
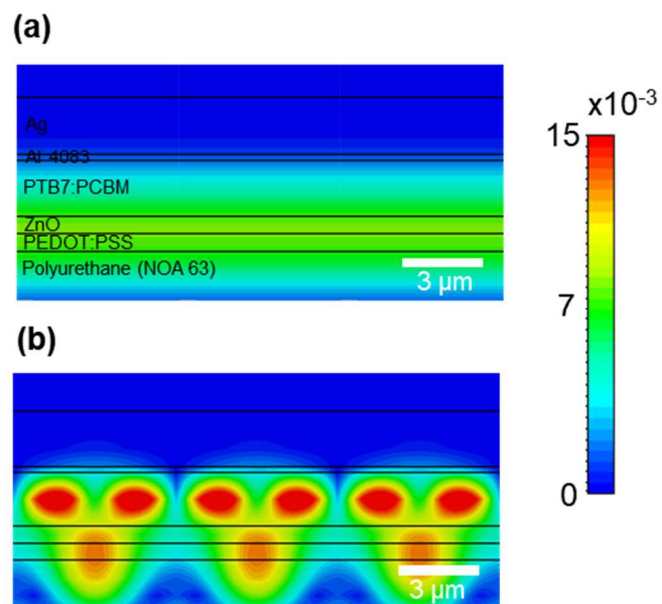
3 µm

x10^{-3}

15

7

0

(b)

3 µm

Figure S9. Electric field distributions of (a) flat and (b) AR 0.7 MCA films for flexible OSCs devices under an illumination of 730 nm based on the peak absorption of PTB7.
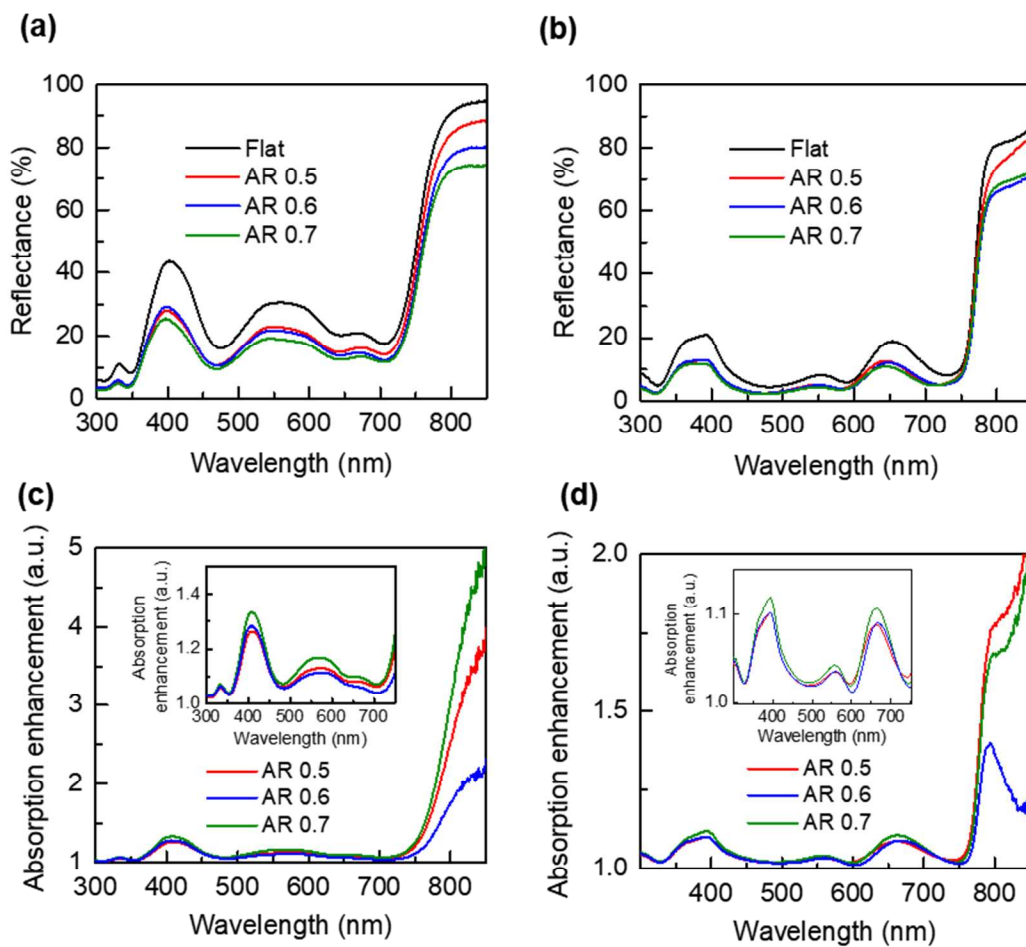
Figure S10. Reflectance spectra of (a) OSCs and (b) PSCs. Absorption enhancement of (c) OSCs and (d) PSCs of a full configuration device structure of flat and various MCA-textured films attached on the ITO/glass back surface.
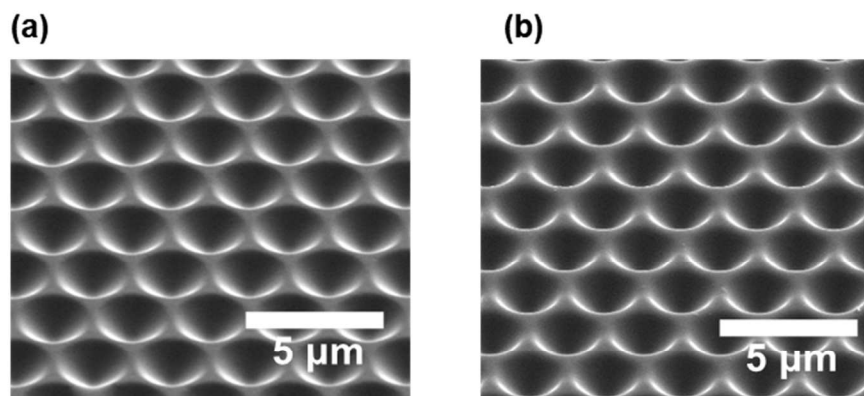
Figure S11. FESEM top images of flexible MCA-OSCs device (a) before and (b) after bending testing of 2,000 cycles.

References

1. Li, K.; Zhang, Y.; Zhen, H.; Wang, H.; Liu, S.; Yan, F.; Zheng, Z. Versatile biomimetic haze films for efficiency enhancement of photovoltaic devices. *J. Mater. Chem. A* **2017,** *5* (3), 969-974.